CHARACTERISATION OF MECHANICAL PROPERTIES OF MULTIPASS SUBMERGED ARC WELD BY MODEL ANALYSIS OF ITS MICROSTRUCTURE FACILITATED BY AID OF COMPUTER

P. K. Ghosh and Maqsood Ahmed
Welding Research Laboratory
Department of Mechanical & Industrial Engineering
University of Roorkee, Roorkee-247 667, INDIA.

ABSTRACT

An analytical model for quantitative analysis of microstructural constituents of a multipass weld produced by consumable electrode process, such as the fraction of dendritic and reheat refined zones in the matrix, has been proposed. The universality of the proposed model has been justified by its applicability for a multipass weld deposit of any material, with due consideration of its physical properties relevant to the operation of the model expressions at appropriate steps of analysis. Empirical correlations of some mechanical propertiesof multipass weld of C-Mn steel with its dendrite content have been developed by preparing a data bank on the reported results. On the basis of the mathematical model expressions and the empirical relationships a user's friendly PC based software has been developed using C language to estimate the microstructural constituents of a multipass weld prepared at given welding parameters and its mechanical properties. The data base of the empirical relationship for prediction of mechanical properties of a multipass weld has been kept flexible for updating by incorporation of new data in it. The validity of estimated characteristics of a multipass submerged arc weld of C-Mn steel, such as its bead geometry, morphology and mechanical properties, deposited at different welding parameters has been verified with a number of experimental data reported by earlier workers as well as with those produced in this work. The ready usage of the model expressions for analysis of the weld characteristics using the welding parameters reported by various workers shows the versatility of the proposed analytical model and the software.

INTRODUCTION

The multipass submerged arc welding (SAW) is widely used in various industries as a vital process for welding of thick plates and pipes of different structural steels due to its ability to produce good quality weld with high deposition rate [1-3]. The SAW is preferably used with a basic flux and DC power source, though in some cases an AC power source is also used [4]. Mechanical properties of a multipass weld is largely governed by its complex microstructural features [5-14], broadly consist of the regions of columnar dendrites and reheat refined grains [8,9,15,16]. Thus, the quality assurance of a thick multipass weld, satisfying its desired properties, should primarily be made by controlling the fraction of micro level features of matrix morphology of the weld. The presence of coaxial columnar dendrites in the matrix also introduces microstructural anisotropy in a thick multipass weld and consequently provides anisotropy in its mechanical properties. Taking into consideration the anisotropy of a multipass weld its mechanical properties are generally categorised in three directions [5-7] as longitudinal (L), transverse (T) and short transverse (S) with respect to the direction of welding marked as L-direction, as shown in Fig. 1. The degree of anisotropy in mechanical properties varies with the amount of columnar dendrite in the matrix [5-8]. Thus, for characterisation of mechanical properties of a multipass weld right prediction of its microstructure and resulting mechanical properties at a given welding parameter may be of considerable interest to the welding engineers.

The amount of columnar dendrite and reheat refined zones in a multipass weld is largely dictated by the welding parameters [5,9,15] but, quantitative prediction of the microstructural constituents of a multipass weld is highly complex in nature as it depends upon a number of factors, which may be primarily named as the preheating/interpass temperature and welding parameters affecting the energy input and weld bead geometry [9,15,20]. Apart from these factors many other aspects like the size and type of electrode, positioning of electrode, polarity of electrode, physical properties of the depositing weld metal etc. also play a significant role on this matter [8]. Thus, before selection of welding parameters for a multipass weld of desired properties, one in general depends upon experiences of welding engineer and/or extensive trial on test pieces, where the first aspect carries uncertainty due to involvement of human nature, intelligence, instinct, availability, logical bias, error etc. and the second aspect involves cost and time consuming preparation of test welds especially in case of preparation of large welds. In this regard a model analysis of resulting microstructure advocating the desired mechanical properties of a multipas weld prepared under given welding parameters may be of considerable interest to the shop-floor welding engineer. In an earlier work on fundamental aspect of welding some complex model expressions[17], developed through spatial geometric solutions, have been proposed for quantitative analysis of microstructural constituents of a multipass submerged arc weld, broadly indentified as dendritic and reheat refined zone in macro level. However, the expressions have not been found universal and versatile primarily due to their dependence on certain experimental values of weld geometry and non-consideration of some physical properties of weld metal.

The significant development in computer applications, with no exception, is also being employed in the field of welding science and engineering to answer different questions on various aspects of welding. A quickly made complex quantitative analysis of resulting microstructural constituents of a multipass weld, prepared under any welding parameter, is possible only with the aid of computer. This may be very much useful to a shop-floor welding engineer to take a practically flawless and economical decision about the welding parameters resulting in a microstructure advocating the mechanical properties of a multipass weld, which is otherwise generally performed by preparing many expensive trial welds. But hardly any software of such kind is available for this purpose.

In this investigation an effort has been made to develop a universal analytical model, capable to work for any weld metal deposited by consumable electrode welding process, for prediction of micro structure of a multipass weld produced at given welding parameters. The work is primarily based on quantitative estimation of bead geometry and columnar dendrite content of a multipass weld using the mathematical model on the proposed [17] spatial geometric concept of bead deposition. In

Table - I Chemical composition of the filler wire

Chemical composition (wt.%)					
C	Mn	Si	Cu	S	P
0.1-02	1.7-2.2	0.1(max)	0.35(max)	0.35(max)	0.35(max)

Table - II Chemical composition of the basic agglomerated flux

Chemical composition (wt.%)				
SiO_2+TiO_2	CaO+MgO	Al_2O_3+MnO	CaF_2	Basicity Index
10	30	20	35	3.1

Table - III Welding parameters

Welding current (Amp)	Arc voltage (Volt)	Welding speed (cm/min)
450	32	50
550	32	50
650	32	50

Table - IV Comparison of the estimated and experimental results of bead height of submerged arc weld of C-Mn steel deposited at different electrode polarity

Weld Current Amp.	Arc Voltage Volt	Weld Speed cm/min	Wire Dia. mm	Elec. Extn. mm	Bead Height (mm)						Ref.
					DCEN		DCEP		AC		
					Est.	Exp.	Est.	Exp.	Est.	Exp.	
500	30	50	4	40	–	–	3.26	3.3	–	–	17
600	30	50	4	40	–	–	3.77	3.9	–	–	17
600	28	50	4	40	–	–	3.87	4.3	–	–	17
600	35	50	4	40	–	–	3.53	3.7	–	–	17
600	40	50	4	40	–	–	3.33	3.2	–	–	17
600	30	50	4	40	–	–	4.21	4.05	–	–	17
300	28	40	3.15	25	3.55	3.20	2.51	2.7	–	–	24
400	28	40	3.15	25	4.30	3.90	3.15	2.9	–	–	24
500	28	40	3.15	25	5.07	4.20	3.75	3.0	–	–	24
600	28	40	3.15	25	5.65	4.4	4.35	3.2	–	–	24
700	28	40	3.15	25	6.1	5.5	4.90	3.5	–	–	24
350	30	53.5	4	19	3.16	3.2	2.15	2.00	1.96	–	19
450	30	53.5	4	19	3.70	3.0	2.58	2.50	2.61	2.60	19
550	30	53.5	4	19	4.22	4.00	2.90	2.00	3.18	2.95	19
650	30	53.5	4	19	4.70	4.80	3.30	3.00	3.69	5.20	19
750	30	53.5	4	19	5.15	5.60	3.70	3.10	4.15	4.80	19
350	35	53.5	4	19	2.96	2.50	2.01	2.4	1.82	–	19
450	35	53.5	4	19	3.49	2.70	2.41	2.6	2.44	2.50	19
550	35	53.5	4	19	3.98	3.90	2.77	2.7	2.97	2.40	19
650	35	53.5	4	19	4.40	3.10	3.12	2.0	3.46	3.30	19
750	35	53.5	4	19	4.85	4.60	3.46	2.7	3.90	4.50	19

Preheat/Interpass Temperature = 175°C (448K)
DCEP = Direct Current Electrode Positive
DCEN = Direct Current Electrode Negative
AC = Alternating Current

Table - V : Comparison of the estimated and experimental results of the constituents of microstructure of submerged arc weld deposit of C-Mn steel deposited at electrode polarity of DCEP

Weld Current 1Amp.	Arc Voltage Volt	Weld Speed cm/min	Wire Dia. mm	Electd. Extn. mm	Area Fraction (%)				Ref.
					Dendrite (D_f)		Refined HAZ (R_f)		
					Est.	Exp.	Est.	Exp.	
500	30	50	4	40	12.05	17.5	87.95	82.5	5
600	30	50	4	40	16.47	19.5	83.53	80.5	5
600	32	50	4	40	15.3	17.5	84.7	82.5	5
600	30	40	4	40	23.13	22.5	76.87	77.5	5
450	32	50	4	40	9.08	13.0	90.92	87.0	PW
550	32	50	4	40	12.79	15.0	87.21	85.0	PW
650	32	50	4	40	18.36	22.0	81.64	78.0	PW

PW = Present Work

SURARC

LATEST GENERATION WELDING MACHINES FROM THE PIONEER


T-series Fully Thyristor based Rectifier

Move-series CO_2/MIG Welder

SUR IRON has been manufacturing welding machines for more than four decades and is one of the largest manufacturers of arc welding machines in India. Our recent collaboration with **OSAKA DENKI (DAIDEN), JAPAN** reflects our total commitment to our valued customers in serving them with latest products and services.

SURARC PRODUCT RANGE

- AN&AF series Air Cooled AC Welder: 150 – 600 Amps
- XR series D.C. Rectifier Welder: 300 – 600 Amps
- T series Fully Thyristorised D. C. Welder: 350 – 600 Amps
- AFT series A. C. TIG Welder : 300 – 600 Amps.
- GTT series D. C. Thyristorised TIG Welder : 350 – 600 Amps
- ARC star series IGBT Inverters : 160 & 250 Amps
- DWG series diesel engine driven welding generator : 300 – 500 Amps
  - Pedestal Type Spot Welder
  - Move series fully thyristorised CO_2/MIG 250 & 400 Amps manufactured in collaboration with OSAKA DENKI, Japan
  - MECHWELD series automatic submerged ARC Welder : 600, 800 & 1200 Amps
  - Welding Column & Boom, Positioners, Rotators & Custom built welding systems.


FIELDKING DWG series Portable Diesel Engine Driven Welding Generator

SISCO

SUR IRON & STEEL CO. (P) LTD.
15 Convent Road, Calcutta 700014 Phone: 244 8359/1307, 245 4179
Fax: +91(33) 244 1308 Cable: CALSISCO
Mumbai Office : 483 Central Facility, Building - 2, APMC -2,
Sector -19, Vashi, Navi Mumbai 400 705 Phone : (022) 765 8885

AN ELECTRIFYING PERFORMANCE

reference to the dendrite fraction, as one of the two basic constituents of a multipass weld, the tensile, C_v - impact toughness and fatigue crack growth rate properties of submerged arc multipass welds of C-Mn steel have been evaluated by using some empirical expressions worked out on the basis of reported results, correlating the dendrite fraction and various mechanical properties of the welds. A user's friendly software for quality assurance of multipass weld with respect to its mechanical properties have been developed using the proposed mathematical model and the empirical relationships for determining mechanical properties of a multipass weld prepared at given welding parameters.

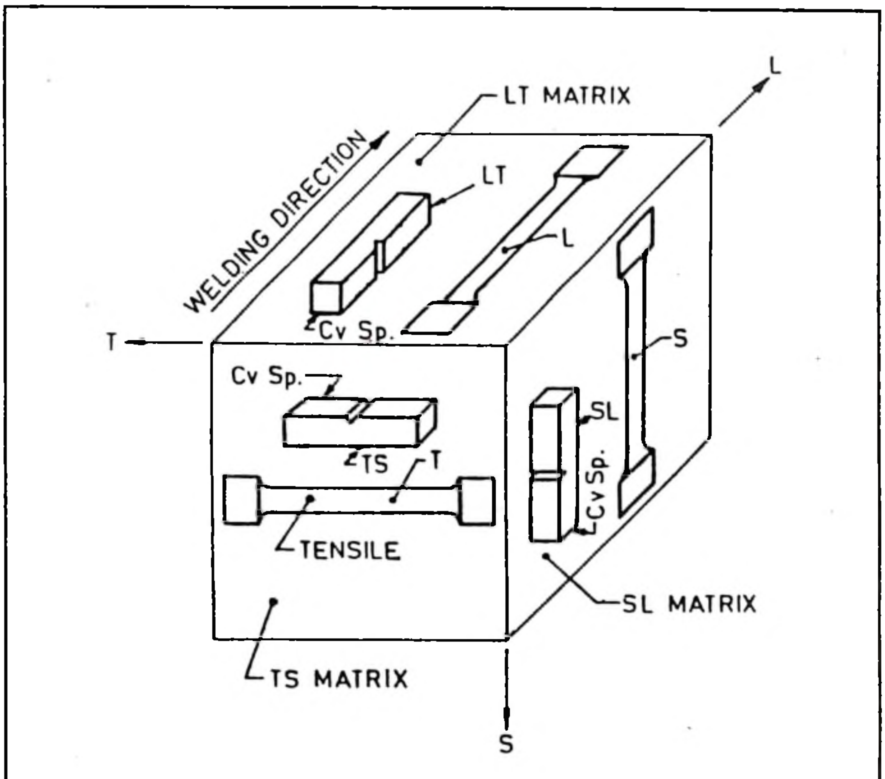

Fig. 1 : Schematic diagram of a multipass weld block showing the orientation of tensile and C_V notch impact tests specimens at its different sections in reference to direction of welding.

METHODOLOGY

Model Analysis of Miocrostructure of a Multipass weld

The experimentally verified model expressions reported earlier [17] for quantitative analysis of weld bead geometry and dendrite fraction of a multipass submerged arc weld have been modified, primarily by eliminating their dependence on experimental values of weld bead geometry, to make them universal and versatile for application in any condition of multipass submerged arc welding of any material. In this model expressions of multipass weldment, the weld beads containing dendrites are assumed to be semicircular in nature with radius r and the HAZ as reheat refined region is considered to be extended up to radius r_1, as schematically depicted in Fig. 2(a and b). The width and height of reinforcement of the weld beads are defined as $2r$ and h respectively. The HAZ is defined as the region up to which a perceptible change in microstructure, comprising recrystallisstion of dendrites is observed. The proposed [17] expression for estimation of r (as stated below), derived by the assumption of heating as a point source due to its large participation in melting of base metal, has been found justified. But, in agreement to an earlier work [21] the expression for estimation of r_1 has been duly modified by considering the thermal conductivity of base metal affecting significantly the change in microstructure of HAZ.

$$r = \sqrt{[(2q/v)/\{\pi e \rho c(T_p - T_0)\}]} \qquad .i$$

$$r = \sqrt{[(2q/v)/\{\pi e \rho c(T_{p1} - T_0)\}]} - r_o \qquad ..ii$$

when,

$$r_0 = \sqrt{[(r_a/e).(\pi.a.r_a/v)^{1/2}]} \qquad ..iii$$

and the thermal diffusivity of the matrix, a , is expressed as

$$a = \lambda/\rho c \qquad ...iv$$

Thus, the eq.(ii) can be resolved as follows.

$$r = \sqrt{[(2q/v)/\{\pi e \rho c(T_{p1} - T_0)\}]} - \sqrt{[(r_a/e).(\pi.a.r_a/v)^{1/2}]} \qquad ..v$$

During submerged arc welding the bead height is largely governed by the melting rate, heat input and welding speed [22]. The melting rate

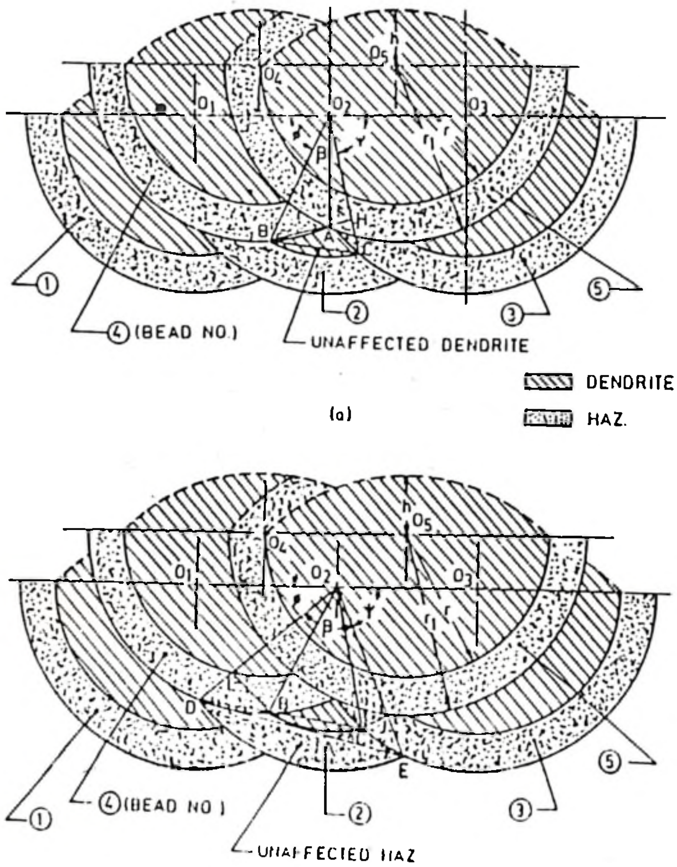

Fig. 2 : Geometric model of a multipass weld (a) for estimation of area fraction of dendrite and (b) for estimation of area fraction of reheat refined HAZ.

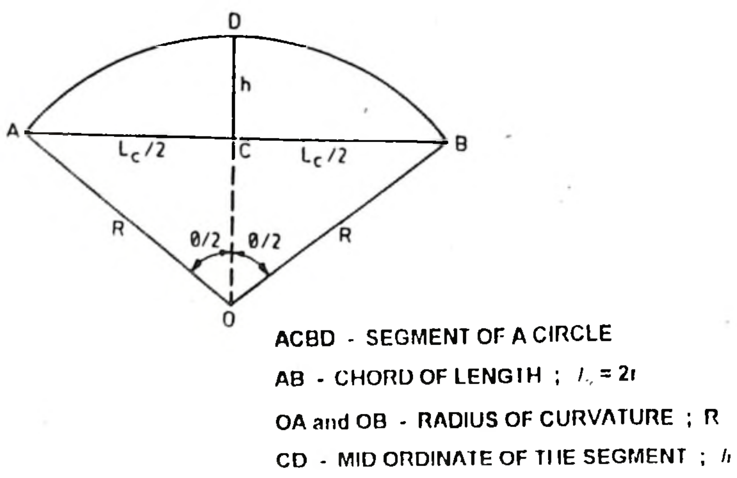

Fig. 3 : Schematic diagram of geometric representation of weld bead reinforcement

of filler wire in submerged arc welding is primarily dependent upon welding variables such as welding current, electrode polarity, wire diameter and electrode extension. At a given wire diameter electrode polarity and electrode extension the melting rate of filler wire enhances with an increase in welding current [23]. It is reported that during welding by consumable electrode process at the electrode polarity of DCEN the melting rate of filler wire becomes higher than that observed when the electrode polarity of DCEP is used [23,24]. However, in case of welding using AC the melting rate of filler wire has been found to lie in between the values obtained during using DCEP and DCEN [23,24]. The melting rate in submerged arc welding at different electrode polarities are expressed [23] as follows

$$\eta_{DCEP} = 0.01037\ E_l + 2.2426 \times 10^{-6}(I^2E_l/d^2) - 0.462 \quad .....vi$$

$$\eta_{DCEN} = 0.016178\ E_l + 2.087 \times 10^{-6}(I^2E_l/d^2) - 0.643 \quad ....vii$$

$$\eta_{AC} = 0.01523\ E_l + 1.6882 \times 10^{-6}(I^2E_l/d^2) - 2.396 \quad ...viii$$

The cross sectional area (A_r) of the weld reinforcement, as a function of volumetric burn-off rate and welding speed, can be expressed as follows

$$A_r = [\eta/(\rho.v)] \quad ..... ix$$

For estimation of bead reinforcement or bead height (h) it is assumed that the weld bead reinforement is segment of a circle of radius R as shown in Fig. 3, where the bead height is the mid-ordinate of the segment. Thus, the area of a bead reinforcement (A_r) can be estimated as area of the segment (A_s) described by a chord (L_c) , which is equal to width of the weld bead. The area of the bead reinforcement and the bead height can be geometrically resolved by the following expressions.

$$A_s = R^2 [\sin^{-1}(L_c/2R) - [\sin \{2\sin^{-1} (L_c / 2R)\}/2]] \qquad \text{........ x}$$

By solving the eqs. (ix) and (x) for $A_r = A_s$ the radius of curvature R can be obtained, which gives rise to estimation of bead height (h) as follows

$$h = R[1-\cos\{\sin^{-1}(L_c / 2R)\}] \qquad \text{....... xi}$$

The primary constituents of the microstructure of a multipass weld, defined above as the regions of columnar dendrites and reheat refined (HAZ) zone of equiaxed grain, can be estimated by the following expressions, valid for $r_1 \leq 2r$, as proposed earlier [17].,

$$\delta = \pi/360 [r^2 \{180 - \sin^{-1} \{(r_1 - h)/r \} - 2\sin^{-1} (r_1/2r)\} - r^2_1 \{180 - \cos^{-1} (r/2r_1) - \sin^{-1} (r_1/2r) - \cos^{-1} (r/r_1)\}]+ (r^2_1 / 2) [\cos\{\cos^{-1}(r/2r_1)\} + \cos\{\sin^{-1}(r_1/2r) + \cos^{-1}(r/r_1)\} - r/2\{\sqrt{4r^2_1 - r^2)/4} - h\} \times \cos \{\sin^{-1} \{(r_1 - h)/r\}\} + \cos \{2\sin^{-1} (r_1 /2r)\}] \qquad \text{.... xii}$$

$$\xi = \pi r^2_1/360 [180-2\cos^{-1}(r/2r_1) - \sin^{-1} \{r_1 -h)/r \} - \cos^{-1} \{\sqrt{(r^2+ 4h^2)} /4r_1 \} + \sin^{-1} \{r\sqrt{(r^2+ 4h^2)}\} + \sin^{-1} \{r\sqrt{(4r^2+ 4^2_1)} / 2r\}] + r\ r_1/2 [\sin \{\cos^{-1}(r/2r_1) - 2\sin^{-1}(r_1/2r) - \sin [\sin^{-1}\{2h /\sqrt{r^2 + 4h^2)}\} + \sin^{-1} \{(r_1 - h)/r)] + r^2_1 / 2 [\sin [\cos^{-1} (r/2r_1) - \sin^{-1} \{\sqrt{(4r^2 - r^2_1)} / 2r \}] + \sin [\cos^{-1} \{\sqrt{(r^2 + 4h^2)} / 4r_1\} - \sin^{-1} \{r/\sqrt{(r^2 +4h^2)}\} - \sin [\cos^{-1} (r/2r_1)+ \sin^{-1} \{(r_1 - h)/r\}]] + \cos^{-1} \{\sqrt{(r^2 + 4h^2)} / 4r1\} \qquad \text{.... xiii}$$

Where, the δ and ξ are the areas of unaffected dendrite (ABC) and reheat refined region (BCED) retained in the matrix as a result of interaction of four weld beads at any sector of a multipass weld, as shown in Fig. 2 (a) and (b) respectively. Thus, the area fractions of dendrite (D_f) and the reheat refined regions (R_f) in the matrix of the multipass weld can be estimated as

$$Df = [\delta / (\delta + \xi)] \qquad \text{........ xiv}$$

and

$$Rf = [1 - D_f] \qquad \text{........ xv}$$

Correlations of Microstructure and Mechanical Properties

In consideration of the reported results (5,6) the following second-or-

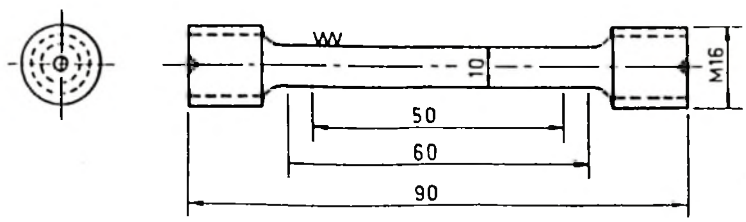

Fig. 4 : Schematic diagram of tensile test specimen

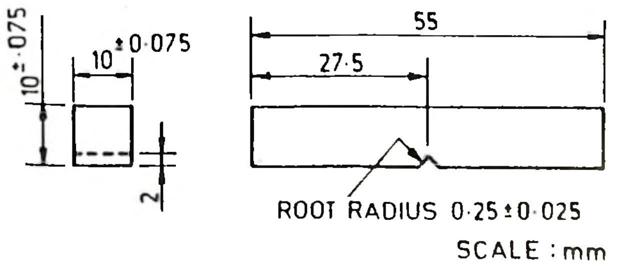

Fig. 5 : Schematic diagram of C_V notch impact test specimens

der polynomial (regression) best fit empirical correlations of the tensile and impact toughness properties with the dendrite fraction of multipass submerged arc welds of C-Mn steel have been developed. Taking into consideration the anisotropy of the welds, in presence of the columnar dendrites, the correlations are also categorised in reference to the L, T and S directions. The nature of empirical correlations for estimation of tensile properties, such as the ultimate tensile strength (σ), yield strength (σy), elongation (e) and Cv -notch impact toughness are worked out as

$$\sigma u = k_{U1} (D_f)^2 - k_{u2} D_f + k_{u3}$$
$$\sigma y = k_{y1} (D_f)^2 - k_{y2} D_f + k_{y3}$$
$$e = (-k_{e1}) (D_f)^2 - k_{e2} D_f + k_{e3}$$
$$Cv = (-k_{i1}) (D_f)^2 - k_{i2} D_f + k_{i3}$$

.... xvi, xvii, xviii, xix

The fatigue crack growth rate (da/dN) of the multipass C-Mn steel weld, at a given stress intensity factor range (ΔK) under stress ratio of 0.1, has also been considered as follows.

$$(da/dN) = 10^{(-0.035\, Df\, -\, 9.278)} \{\Delta K\}^{(0.015\, Df\, +\, 2.663)} \quad \text{.. xx}$$

Where, the (k_{U1}, k_{U2} and k_{U3}), (k_{y1}, k_{y2} and k_{y3}) and (k_{e1}, k_{e2} and k_{e3}) are constants for estimation of the tensile properties and their values change for the properties of different directions as L,T and S. The k_{i1}, k_{i2} and k_{i3} are also constants for estimation of C_V-notch impact toughness of the weld and their values change for estimation of toughness of different directions as the LT, TS and SL (Fig. 1) at different temperatures identified as 27, -20 and -40°C. The expression (xx) which has been developed in an earlier work (25), estimates fatigue crack growth rate in LT direction of a multipass weld at ambient temperature.

Experimentation

Three all weld metal blocks of C-Mn steel of size 150x50x50 mm were prepared by multipass submerged arc welding process, using 4.0 mm diameter filler wire (Grade-C) at DCEP and basic agglomerated flux (Automelt Grade IV) having chemical compositions as given in Tables - I and II respectively. The submerged arc welding was carried out at different welding currents, where the arc voltage and welding speed were kept constant as shown in Table - III and the preheat and interpass temperature was maintained as 175 ±25°C. During multipass deposition the electrode, having a stick out of about 40 mm, was visually positioned in reference to a weld bead deposited earlier, as per standard practice of multipass welding.

For metallographic studies the specimens were collected from middle portion of the all weld blocks and transverse section of the weld, in reference to the direction of welding, was prepared by standard metallographic procedure. The polished surface was etched in 5% alcoholic nitric acid solution and studied under optical microscope for estimation of the area fraction of dendrites by following the standard random linear intercept method.

The tensile and Charpy V-notch impact tougness properties of the all weld deposits were studied using the specimens as schematically shown in Figs. 4 and 5 respectively, confirming the standards of ASTM E8 and ASTM E23 respectively. The tensile and impact test specimens were machined out from the longitudinal (L) and LT directions (Fig. 1) of the all weld block respectively. The tensile test was carried out in a universal testing machine operated at a cross head speed of 1.0 mm/sec. The ultimate tensile strength (σu) and yield strength (σy) was determined on stress-strain diagram plotted by marking the 0.2% off-set strain. The elongation was determined on a gauge length of 40 mm. The tensile test was carried out at room temperature (RT) of 27°C, whereas the Cv-impact test was carried out at 27 and -20°C. The tensile and Cv -notch toughness properties of the weld were studied in L and LT directions respectively, primarily because they are most commonly known directions used for characterisation of all weld deposit, as reported by other workers.

Software for Characterisation of Multipass Weld

In view of the complexity in quantitative analysis of microstructure of a multipass weld a user's friendly PC based software has been developed, using C language on the basis of mathematical models and expressions (i - xv) as stated above, to estimate the dendrite fraction (D_f) of

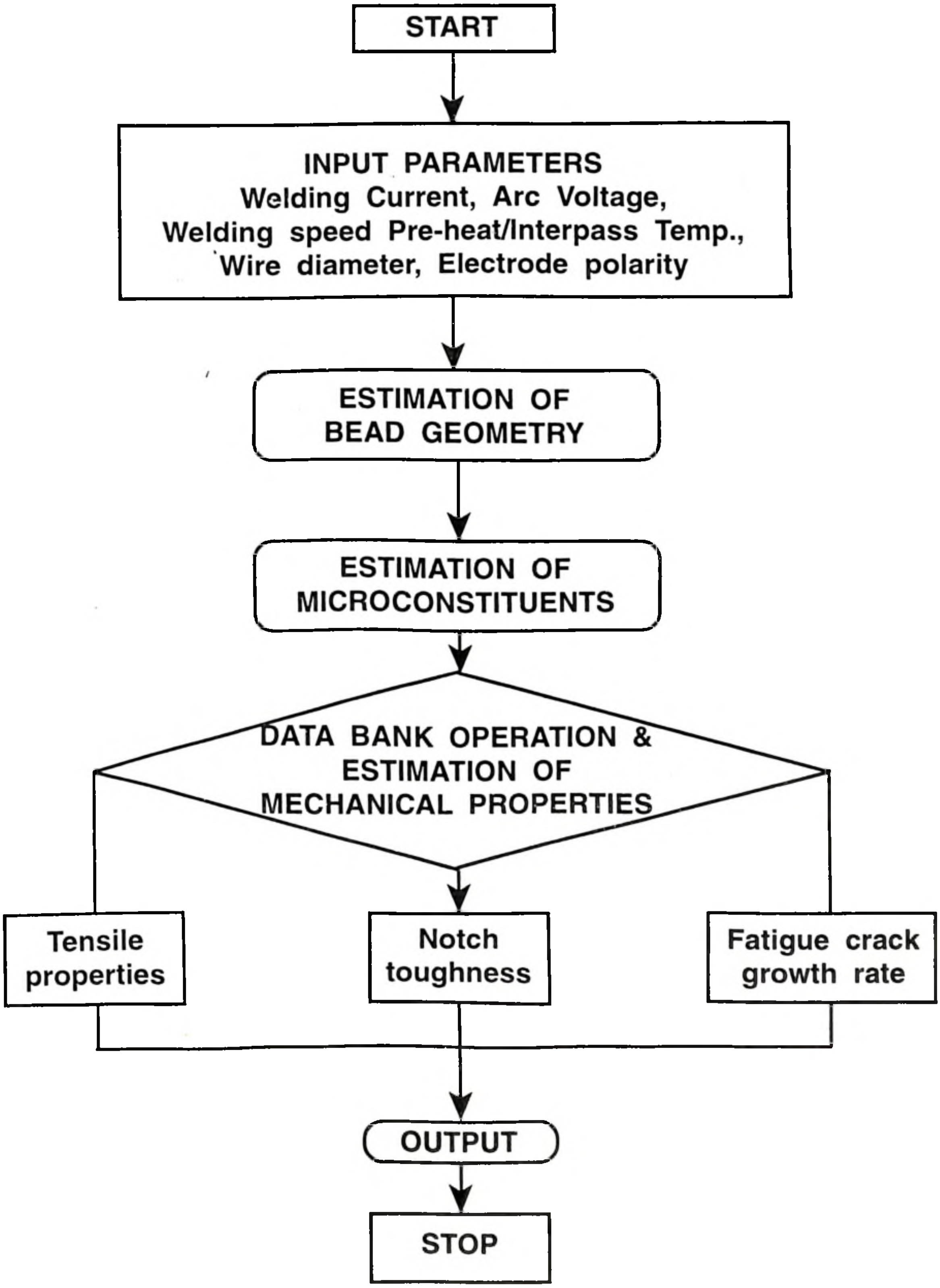

Fig. 6 : Flow Chart of the software

a multipass weld prepared at given welding parameters. The software has also been made capable to estimate the mechanical properties of multipass submerged arc weld of C-Mn steel having chemical composition in the range of 0.1-0.2% C, 1.7-2.2% Mn, 0.1% (max) Si, 0.35% (max) Cu, 0.035% (max) S and 0.35% (max) P, using the empirical relationships (xvi - xx) of various mechanical properties with the D_f of the matrix. The software has been equipped to work for characterisation of mechanical properties of a multipass weld of C-Mn steel, which is of common interest to the welding engineers due to its large applications in various industries. The software has been made user's friendly by keeping input data from well conversant welding parameters such as welding current, arc voltage, welding speed, electrode extension, electrode polarity and preheat/interpass temperature. All these aspects are logically complied in different modules of the software as typically shown in a flow chart presented in Fig. 6. The modules of the software analysing the microstructure of a multipass weld is capable to work for any material produced by any consumable electrode process and the data base of the module giving empirical relationship for prediction of mechanical properties of a multipass weld has been kept flexible for updating by incorporation of new data in it from time to time. The theoretical results are verified with the experimental results reported by various workers.

Verification of Estimated Results

The validity of estimated characteristics of a multipass C-Mn steel weld, such as its bead geometry, microstructure and mechanical properties, deposited at different welding parameters has been verified with a number of experimental data reported by earlier workers as well as with those produced in this work. The typical microstructure of TS section (Fig. 1) of the multipass weld block has been shown in Fig. 7. The ready usage of the model expressions for analysis of the weld characteristics using the welding parameters reported by various workers shows universality of the proposed analytical model.

At different welding parameters and electrode polarities the bead height of weld deposits estimated by the analytical model has been compared with those reported by earlier workers [17,19,24] as shown in Table - IV. The table depicts that the results estimated by the analytical model are in close approximation to those of the experimental results with a difference lying in the range of 10±2.5%. The table also reveals that the analytical model works fairly well for estimation of bead height of submerged arc weld deposit produced at any electrode polarity of DCEP, DCEN and AC.

A comparison of the analytically estimated and experimentally observed area fractions of dendrite (D_f) and reheat refined heat affected zone (R_f) in a multipass weld of C-Mn steel has been shown in Table - V. The table shows that at a given welding parameter the estimated amounts of these micro-constituents of weld deposit obtained by using the analytical model expressions (i - xv) are also in close approximation to the experimentally observed values of them, as reported earlier [5]

Fig. 7 : Typical microstructure of TS section of a multipass submerged arc weld block of C-Mn steel

Table - VI : Comparison of the estimated and experimental results of mechanical properties of a multipass submerged arc weld deposit of C-Mn steel

WC Amp	AV Volt	WS cm/ min	EE mm	UTS MPa Est.	Exp.	YS Mpa Est.	Exp.	El. % Est.	Exp.	C_V-Notch Toughness (J) (RT) Est.	Exp.	-20°C Est.	Exp.	-40°C Est.	Exp.	Ref.
500	30	50	40	545	535	441	430	30	30	113	105	52	55	37	39	5
600	30	50	40	533	537	441	432	29	29	118	120	62	66	43	48	5
600	32	50	40	535	536	441	437	30	28	117	113	60	55	42	37	5
600	30	40	40	531	550	443	438	30	29	121	126	70	63	47	47	5
420	30	45	30	560	555	442	469	31	25	107	–	41	–	30	–	26*
490	32	45	30	552	600	442	517	30	24	110	68	47	47	34	–	26*
500	28	40	30	537	518	441	380	30	26	116	–	58	–	41	–	27
700	28	40	30	546	525	452	395	30	27	120	–	69	–	45	–	27
450	32	50	40	559	528	442	386	31	30	107	128	42	–	–	–	PW
550	32	50	40	542	515	441	388	30	29	114	132	54	62	38	–	PW
650	32	50	40	531	510	441	380	30	30	119	134	65	74	45	–	PW

Electrode Wire Diameter = 4 mm (*3.125 mm)
Electrode Polarity = DCEP
Preheat/Interpass Temp. = 448K

WC = Welding Current
WS = Welding Speed
AV = Arc Voltage

YS = Yield Strength
El. = Elongation
UTS = Ultimate Tensile Strength

and observed in present work (PW), with a variation lying within about 6.0%. In consideration of the closely comparable estimated and experimental results regarding the bead height (Table - IV) and the microstructural constituents (Table - V) of a weld bead or a multipass weld deposit respectively, it may be inferred that the use of the proposed analytical model is justified for characterisation of a multipass weld deposit of any material, with due consideration of its physical properties relevant to the operation of the model expressions at appropriate steps of analysis.

A comparison of the estimated and experimetal results of the tensile and C_V-impact toughness properties of multipass weld deposits of C-Mn steel, produced at different welding parameters has been presented in Table - VI. The table shows that the experimentally observed values of ultimate tensile strength, yield strength and elongation of L direction and C_V-impact toughness of LT direction of a multipass weld, as reported by earlier workers [5,26,27] and also found in present work (PW), are practically well in agreement to their counterparts estimated by the empirical correlations stated in the expressions (xvi)-(xix). The estimated fatigue crack growth rate in LT direction of the weld has also been found in agreement to the measured values of the weld as reported earlier [25]. However, to improve the confidence of using this approach towards characterising mechanical properties of a multipass weld it has to be verified further with more experimental data available in future.

CONCLUSIONS

The proposed analytical model expressions for analysis of the microstructural characteristics of a multipass weld has been found universal due to its ready usage to any weld deposit of consumable electrode process, with due consideration of its physical properties relevant to the operation of the model expressions at appropriate steps of analysis. The user's friendly PC based software developed to carry out the complex analysis of microstructure of a multipass weld and to execute the operation of data base for estimation of mechanical properties of a multipass weld of C-Mn steel using their empirical relationship with the matrix microstructure has been found quite effective. The software has been kept flexible for updating its data bank regarding the mechanical properties of a multipass weld by incorporation of new data in it from time to time. The theoretical results estimated by the software are found significantly well in agreement to the experimental results reported by various workers.

Nomenclature

h = Bead height (mm)

R = Radius of curvature

L_C = Length of Chord (2r)

η = Melting rate at any electrode polarity (kg/hr)

d = Electrode diameter (mm)

E_l = Electrode extension (mm)

T_p = Maximum temperature (K) required for melting of base material during welding

T_{p1} = Maximum temperature (K) required for initiating microstructural change in base material

To = Initial preheat temperature (K)

q = Arc Power, [(VxI)/v], (J/sec)

V = Arc voltage (V)

I = Welding current (A)

ν = Welding speed (m/sec)

r_a = Beam radius (mm) which is proportional to welding electrode

λ = Thermal conductivity of material (J/m/s/K)

a = Thermal diffusivity (m^2/sec)

ρ = Density of weld metal (kg/m^3)

ρc = Volume thermal capacity or specific heat per unit volume ($J/m^3/K$)

e = Base of natural log (2.718)

a = Crack length

N = Number of cycle of dynamic loading

REFERENCES

1. Welding Hand Book, Vol.II, American Welding Society, 7th edition, (1977).
2. H.B. Carry, Modern Welding Technology, Prentice Hall, (1979).
3. B. Laing, R. Heid and A. Pollack, Narrow gap welding of HY-100 plate using closed loop, adaptive feedback, through-the-arc tracking technology, Welding Journal, 64, 11(1985), pp. 38-42.
4. D.D. Swhemmer, D.L. Coloson and D.L. Williamson, Relationships of weld penetration to welding flux, Welding Journal, 58, (1979), pp. 153-160s.
5. P. Yongyuth, P.K. Ghosh, P.C. Gupta, A.K. Patwardhan and S. Prakash, Influence of macrostructure on tensile properties of multipass SAW C-Mn steel deposit, Mater. Trans. JIM, 34, 6(1993), pp. 533-540.
6. P. Yongyuth, P.K. Ghosh, P.C. Gupta, A.K. Patwardhan and S. Prakash, Influence of macro/microstructure on the toughness of all weld multipass submerged arc welded C-Mn steel deposits, ISIJ Int., 32, 6(1992), pp. 771-778.
7. P.K. Ghosh, P. Nagesh Babu and P.C. Gupta, Microstructure-fatigue crack growth rate correlation in multipass submerged arc C-Mn steel weld deposit, ISIJ International, 34, 3(1994), pp. 280-284.
8. G.M. Evans, The effect of heat input on the microstructure and properties of C-Mn all weld metal deposits, Welding Journal, 61, 4(1982), pp. 125-132s.
9. P.K. Ghosh, P.K. Singh and N.B. Potluri, Fracture properties of multipass submerged arc weld of HSLA steel produced by using flux cored filler wire, ISIJ Int., 38, 12(1998), pp. 1379-1386.
10. S.S. Struck and R.D. Stout, Heat treatment effects in multipass weldments of a high strength steel, Welding Journal, 51, 10(1972), pp. 508-520s.
11. G.M. Evans, The effect of carbon on the microstructure and properties of C-Mn all weld metal deposits, Welding Journal, 62, 11(1983), pp. 313-320s.
12. Jose Vercesi and Estela Surian, Effect of welding parameters on high strength SAW all weld metal - Part-I : AWS E 11018-M, Welding Journal, 75, 6(1996), pp. 191.196s.
13. B. Augland and N. Christen, Some observations on the notch toughness of submerged arc weld deposits, Brit, Welding Journal, Oct.(1961), pp. 473-476.
14. J.H. Chen, T.D. Xia and C. Yan, Study on impact toughness of C-Mn multi layer weld metal at -60°C, Welding Journal, 72, 1(1993), pp. 19-27s.
15. K. Millon Hantsch and H. Zimmorian, Submerged arc narrow gap welding of thick welded components, Welding Journal, 61, 7(1982), pp. 27-34.
16. Kenneth Easterling, Introduction to the physical metallurgy of welding, Butterworth, (1983).
17. P.K. Ghosh, P. Yongyuth, P.C. Gupta, A.K. Patwardhan and Satya Prakash, Two dimensional spatial geometric solution for estimating the macroconstituents affecting the mechanical properties of multipass C-Mn steel SAW deposits, ISIJ Int., 35, 1(1995), pp.63-70.
18. B.G. Renwick and B.M. Patchett, Operating characteristics of the

submerged arc welding process, Welding Journal, 55, (1976), pp. 69-76s.

19. P.A. Draptan, Examination of influence of process parameters on submerged arc welding, Weld. Res. Int., 2, 2(1972), pp. 1-20.

20. C.E. Jackson, The science of arc welding, Part-II-consumable electrode welding arc, Welding Journal, 39, 5(1960), pp.177s.

21. J.C. Ion, K.E. Easterling and M.F. Ashby, A second report on diagrams of microstructure and hardness for heat-affected zones on welds, Acta. Metall., 32, 11(1984), pp. 1954-1962.

22. J.F. Lancaster, Physics of welding, International Institute of Welding, Pergamon Press.

23. R.S. Chandel, Mathematical modelling of melting rates for submerged arc welding, Welding Journal, 66, 5(1987), pp. 135-140s.

24. P.C. Gupta, P.K. Ghosh and S.K. Sharma, Effect of polarity on melting rate in submerged arc welding, Ind. Weld. J., 19, 3(1987), pp. 228-233.

25. P.K. Ghosh, Potluri Nagesh Babu and P.C. Gupta, Microstructure-fatigue crack growth rate correlation in multipass submerged arc C-Mn steel weld deposits, ISIJ Int., 34, 3(1994), pp. 280-284.

26. S.S. Tuliani, T. Boniszewski and N.F. Eaton, Notch toughness of commercial submerged-arc weld metal, Welding & Metal Fabrication, 37, 8(1969), pp. 327-339.

27. Dharmendra Singh, Effect of welding parameters on fatigue properties of pure weld metal, M.E. Dissertation. Deptt. Mech. & Ind. Engg., Univ. of Roorkee, (1989).